Available online at www.sciencedirect.com
SCIENCE DIRECT
Diamond & Related Materials 15 (2006) 952 – 957
DIAMOND AND RELATED MATERIALS
www.elsevier.com/locate/diamond

# Improvement of adhesion strength of amorphous carbon films on tungsten ion implanted 321 stainless steel substrate

Ming Xu [a], Liuhe Li [a,b], Xun Cai [a,*], Youming Liu [a,c], Qiulong Chen [a], Paul K. Chu [c,*]

[a] School of Materials Science and Engineering, Shanghai Jiao Tong University, Shanghai 200030, China
[b] 702 Department, Mechanical Engineering School of Beijing University of Aeronautic and Astronautic, 100083, China
[c] Department of Physics and Materials Science, City University of Hong Kong, Kowloon, Hong Kong

Available online 10 January 2006

**Abstract**

Amorphous carbon (a-C) films have many potential applications due to their good mechanical properties. However, poor adhesion on substrates such as tool steels limits its applications. In the present work, a-C films were deposited on W-implanted (20 kV, $3 \times 10^{17}$ ions-cm$^{-2}$) steel substrates by means of plasma immersion ion implantation and deposition (PIII&D). Compared to the films deposited on untreated steel substrates, the films deposited on the W-implanted steel substrates exhibit improved hardness, surface morphology, and adhesion strength. The modified layer with graded mechanical properties not only provides a structural continuity from the substrate to the film but also acts as the interlayer to mitigate stress concentration under applied loads.
© 2005 Elsevier B.V. All rights reserved.

*PACS:* 68.35; 68.55; 62.20; 81.20
*Keywords:* DLC applications; a-C films; Adhesion strength; Tungsten implantation; 321 stainless steel; Nano-scratch

## 1. Introduction

Amorphous carbon (a-C) thin films have found many applications in many areas such as microelectronic and optical devices, biomedical products, corrosion resistant materials, protective overcoats, as well as microelectro-mechanical systems (MEMS) [1–5]. Properties that determine the applicability of a-C films include not only the typical mechanical aspects such as hardness and elastic modulus but also the adhesion strength between the films and substrates. Multilayer preparation [6,7] and interlayer deposition [8] are two common methods to improve the adhesion strength. To our knowledge, there have been few reports on pre-treating the substrate by ion implantation to improve the film adhesion strength. As demands for a-C technology are getting wider and more stringent, such as large area processing and deposition onto complex-shaped components, more versatile and universally applicable processing methods need to be developed.

In this work, we investigate the improvement rendered by tungsten pre-implantation into 321 stainless steel substrates prior to the deposition of a-C films. Due to the excellent chemical affinity between tungsten and carbon, a modified layer with the co-existence of WC and C forms on the substrate surface. This layer offers better film adherence and load bearing capacities.

## 2. Experimental details

Coupons of 321 stainless steels (composition in wt.%: Fe—70.1, C—0.11, Si—0.90, Cr—18.2, Ni—9.40, Ti—0.64, S—0.06, and P—0.03) were cut into dimensions of $15 \times 15 \times 2$ mm$^3$. The samples were austenized at 1500 K for one hour to achieve a solid solution state. They were then polished and cleaned with acetone before treatments.

Tungsten ion implantation was carried out in a multi-purpose plasma immersion ion implanter (PIII) equipped with several plasma generating tools including RF discharge, hot filament discharge, and vacuum arc metal plasma sources [9–11]. The base pressure in the vacuum chamber was $3 \times 10^{-3}$ Pa.

* Corresponding authors. Chu is to be contacted at Department of Physics and Materials Science, City University of Hong Kong, Kowloon, Hong Kong. Tel.: +852 27887724; fax: +852 27889549. Cai, School of Materials Science and Engineering, Shanghai Jiao Tong University, Shanghai 200030, China. Tel.: +86 21 62932087.
*E-mail addresses:* xcai@sjtu.edu.cn (X. Cai), paul.chu@cityu.edu.hk (P.K. Chu).

0925-9635/$ - see front matter © 2005 Elsevier B.V. All rights reserved.
doi:10.1016/j.diamond.2005.11.005

Tungsten PIII was conducted using the following conditions: Target bias $V_i$=20 kV; Main arc average current $I_a$=1.0 A; Pulse repetition rate $f$=40 Hz. Samples 1 and 2 underwent W PIII for about an hour to achieve an approximate implant fluence of $3\times10^{17}$ ions-cm$^{-2}$. Synchronization of the target bias and vacuum arc pulses ensured pure metal PIII without significant metal deposition. After W PIII, $C_2H_2$ was introduced into the vacuum chamber and RF discharge was formed inside the vacuum chamber to ignite the plasma. In this mode, a-C thin films can be deposited using plasma immersion ion implantation and deposition (PIII&D) without breaking vacuum thereby eliminating potential contamination during sample transfer. In PIII&D, the $C_2H_2$ plasma was also sustained by 1 kW hot filament discharge. Negative high voltage (−20 kV) pulses with a pulse width of 400 μs were applied to the W-implanted substrate (sample 2) at a repetitive frequency of 40 Hz. The processing time was 4 h and the a-C film thickness was approximately 0.5 μm. Sample 3 was prepared by conducting a-C film deposition directly onto the untreated steel substrate under similar PIII&D conditions as sample 2.

X-ray photoelectron spectroscopy (XPS) was employed to investigate the composition and chemical bonding of the W ion-implanted 321 stainless steel sample (sample 1). Elemental depth profiles were acquired using argon ion bombardment at an approximate sputtering rate of 4.7 nm/min. The change of structure and phases in the near surface in comparison with the untreated 321 steel substrate was determined by X-ray diffraction.

The structure of the a-C films on samples 2 and 3 was analyzed by Raman spectroscopy. The hardness was obtained by nanoindentation measurements using a CSM three-sided pyramidal diamond (Berkovich) indenter with options for continuous stiffness measurement. A series of indentations were performed at loads of 0.5, 1, 2 and 4 mN. Five indents were averaged to determine the mean H and E values of each load for statistical purpose.

The adhesion properties of the a-C films were assessed with a nano-scratch test performed with a different diamond indenter (taper indenter with 2 μm radius) on the face direction in order to delaminate the films. 700 μm scratching tracks were made on the samples 2 and 3. The system had a load (displacement) resolution of 50 nN (<0.01 nm). Experiments were performed in a clean-air environment of ~45% relative humidity at an ambient temperature of 22(±1) °C. The normal load of the indenter was linearly ramped from the minimum to the maximum during scratching and the maximum loads were 10 and 30 mN, respectively. The sample surfaces were examined by optical microscopy after the test. The coefficients of friction were calculated using a technique that has been reported elsewhere [12].

## 3. Results

Fig. 1 displays the XPS elemental depth profile acquired from the steel substrate after W PIII. The tungsten profile shows a typical 'implant-like' Gaussian distribution, implying that pure tungsten ion implantation has been achieved. Due to its chemical affinity with carbon, a large amount of carbon is also found on the substrate surface.

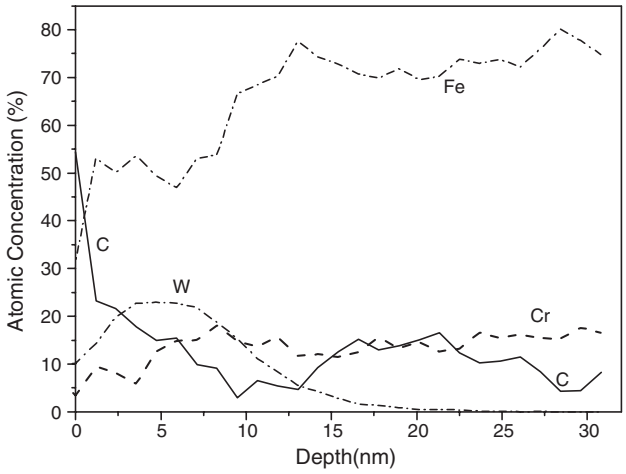


Fig. 1. XPS depth profile of the steel substrate implanted with $W^+$ ions (20 kV, $3\times10^{17}$ ions-cm$^{-2}$).

The high-resolution C1s, Fe2p and W4f XPS spectra are exhibited in Fig. 2. The W4f spectrum reveals the $W4f_{7/2}$ doublet corresponding to carbide-modified tungsten [13,14]. One of the two C1s peaks centered at 283.3 eV is associated with C–W bonding [15]. The other peak at 284.4 eV indicates the presence of C–C bonding or graphitic C corresponding to $sp^2$ [16–18]. The Fe2p peaks corresponding to α-Fe are observed at 720.1 and 706.9 eV [19–21]. According to Porte [22], the binding energies of Fe2p electrons are affected by tungsten atoms in the vicinity so that the values are slightly lower than that of pure iron. For comparison, XRD was also performed on the untreated substrate and the results are shown in Fig. 3. Only the diffraction peaks of α-Fe can be observed in the pattern suggesting that no carbide phase exists in the untreated substrate. The presence of $Fe_2TiO_4$ results from the sample oxidation in the XRD examination.

Fig. 4(a) and (b) show the Raman spectra of the a-C films on the W PIII and untreated 321 stainless steel samples, respectively. By using Gaussian multi-peak fitting, both of the Raman spectra can be deconvoluted into two sub-peaks: G band at 1560 cm$^{-1}$ and D band at approximately 1360 cm$^{-1}$. Because of the same deposition conditions, the two a-C films yield similar Raman spectra. In this work, the a-C films were deposited using mixed argon and $C_2H_2$ so that the C=C bonds can be the predominating factor on the higher D Raman peak, implying a larger domain size of the $sp^2$ clusters. Our results show that owing to the same preparation parameters, the two samples have similar film structures that are not modified by the different substrate surfaces.

The nanohardness of samples 2 and 3 as a function of loads (mN) is shown in Fig. 5. The hardness values vary inversely with the loads. Because of small film thickness (0.5 μm), the hardness is affected by the film as well as the substrate. The hardness of the a-C film on the W-implanted substrate increases from 10 to 15 GPa. The formation of the strengthened phase WC detected by XPS is believed to be the cause for the hardness improvement.

Nano-scratch tests were conducted to examine the general scratch behavior of the a-C films and to quantify their scratch resistance. Fig. 6(a)–(d) show the coefficient of friction ($\mu$) as a function of the normal ramping load and scratch length. Fig. 7(a)–(d) depict the 200× optical micrographs of the scratch tracks. Five scratches were made for each load on different locations of each sample for good statistics. The coefficient of friction $\mu$ is calculated by taking the ratio of the lateral force and normal load on the indenter. Until the tip begins to slide with respect to the sample surface, $\mu$ cannot be determined. At the start of the scratch, the lateral force data is noisy indicating a stick-slip phenomenon (Fig. 6). Once the normal load reaches about 0.5 mN, $\mu$ settles to nearly constant values. As shown in Fig. 6(a) and (b), the nano-scratch results obtained from the a-C film deposited on the untreated substrate indicate poor

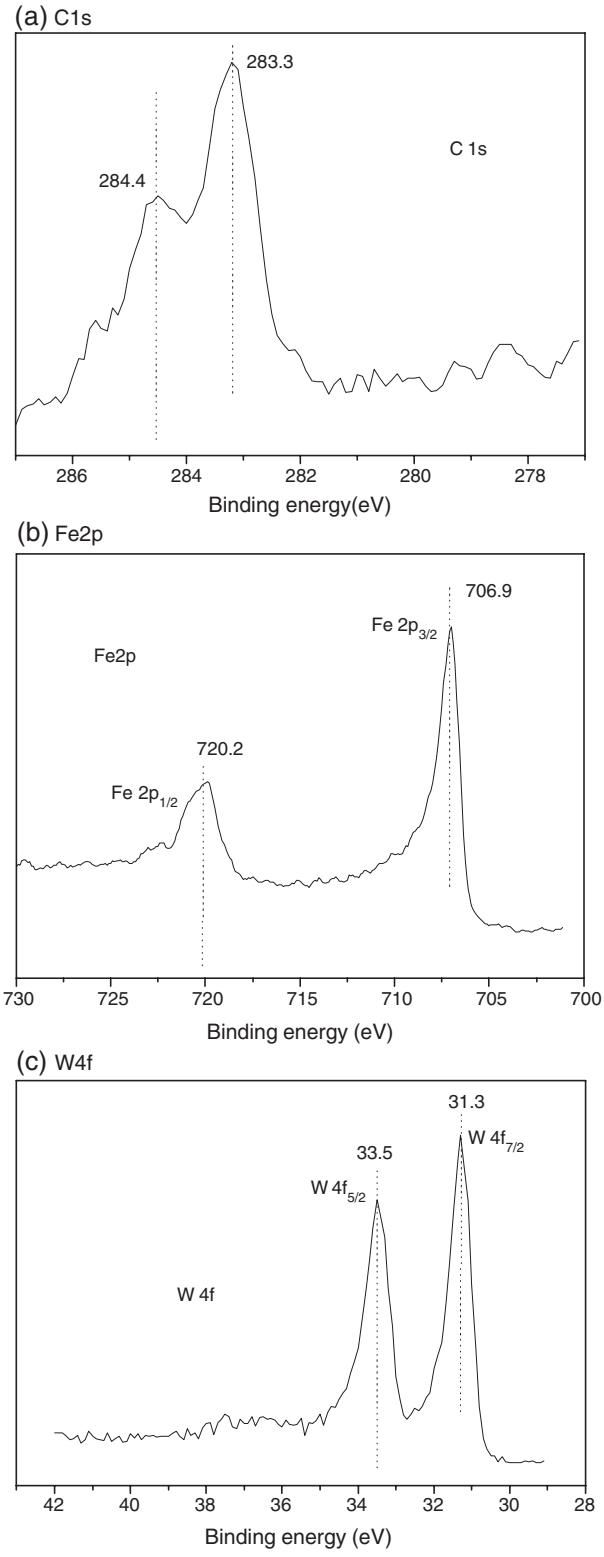


Fig. 2. High-resolution XPS spectra: (a) C1s, (b) Fe2p, and (c) W4f.

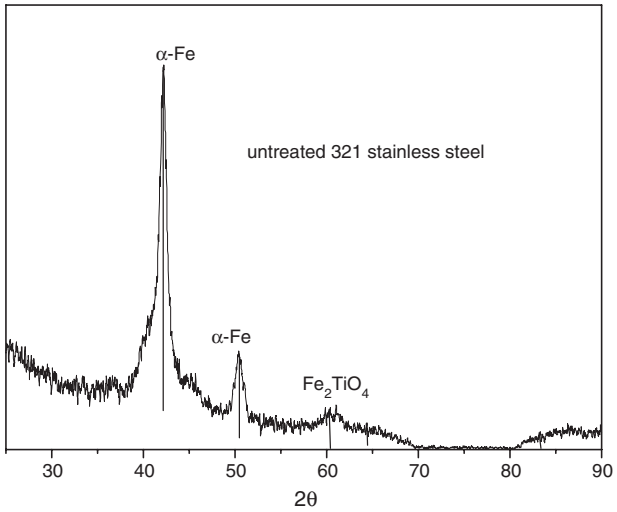


Fig. 3. XRD pattern of untreated 321 stainless steel sample.

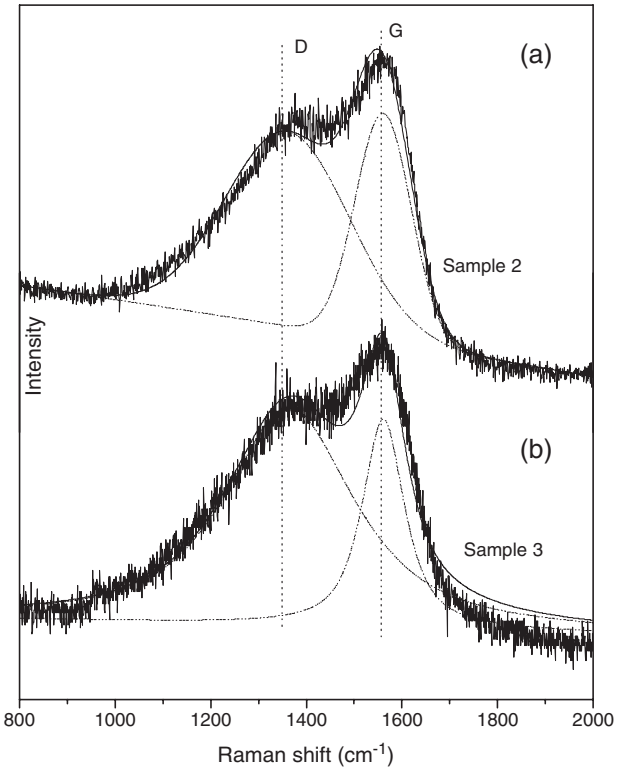


Fig. 4. Raman spectra acquired from: (a) sample 2: a-C film deposited on $W^+$-implanted 321 stainless steel and (b) sample 3: a-C film deposited on the untreated 321 stainless steel.

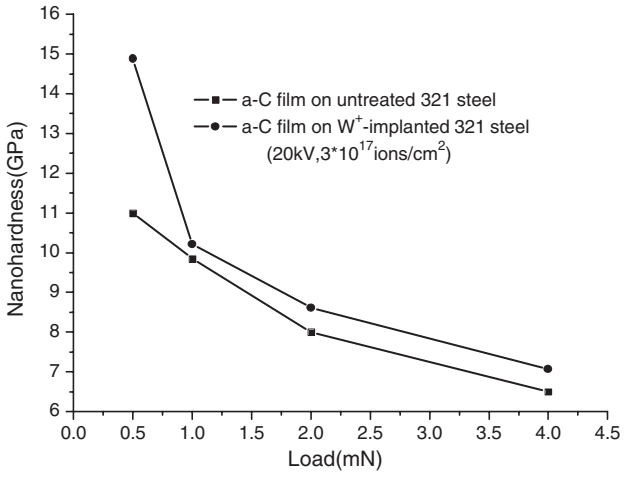


Fig. 5. Nanohardness of a-C films (samples 2 and 3).

adhesion. At the maximum load of 10 mN, the steel substrate begins to produce cracks and small regions of delamination can be seen at the 450 μm scratch path (above the load of 8 mN). The scratch tracks shown in Fig. 7(a) reveal abrupt changes in $\mu$ marked by C in Fig. 6(b) (load of 13 mN). Failure manifests in brittle fragmentation of the film. Significant film delamination can be observed from the exposed area in Fig.7(b) probably due to tensile-type cracks. When the substrate is pretreated with W PIII, the adhesion strength is improved as shown in Fig. 6(c) and (d). The friction coefficient maintains a stable value of 0.2 [Fig. 6(c)] and no fracture can be found from the scratch tracks in Fig. 7(c). Only when the load is higher than 20 mN (marked in Fig. 6(d)) then $\mu$ exhibits fluctuation corresponding to the film fracture morphology in Fig. 7(d).

## 4. Discussion

W pre-implantation creates a modified layer in which carbon, tungsten and other substrate elements coexist and as indicated by our XPS results, tungsten carbide and C–C bonds are formed on the steel substrate prior to a-C film deposition. The formation of the strengthened phase of WC leads to enhanced hardness of the substrate. Dyrda and Sayer [23] and Hu and Tu [24] have suggested that the harder the substrate, the better the film adhesion to the substrate. Hence, in our treated samples, the improved hardness provides more effective support to bear loads and withstand scratches.

Loading always causes increased elastic and plastic deformation finally resulting in failure in the surface region [25]. This failure is most likely due to film delamination at the interface where the mechanical characteristics are usually the worst. The modified layer with gradient properties, especially with the presence of graphite C, can provide a lattice-matched

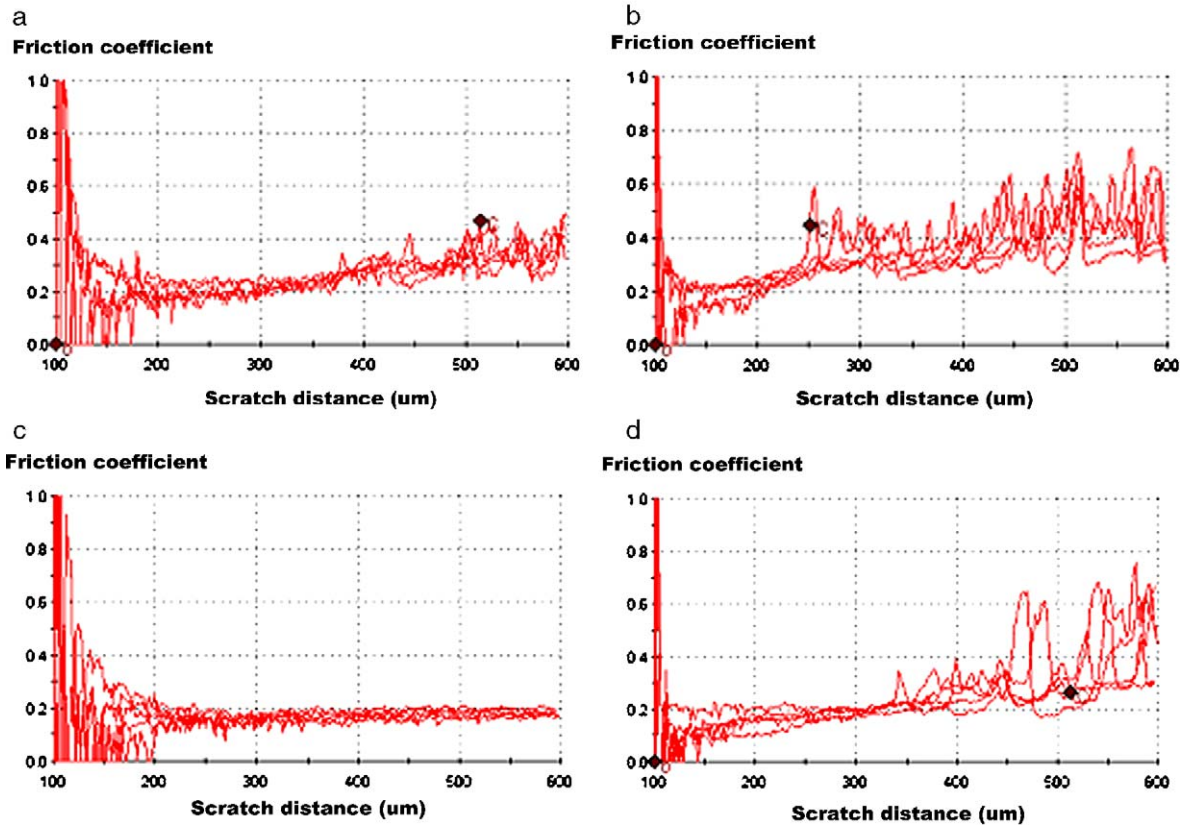


Fig. 6. Coefficient of friction profiles: (a) a-C film deposited on untreated substrate at a maximum load of 10 mN, (b) a-C film deposited on untreated substrate at a maximum load of 30 mN, (c) a-C film deposited on $W^+$-implanted substrate at a maximum load of 10 mN, and (d) a-C film deposited on $W^+$-implanted substrate at a maximum load of 30 mN.

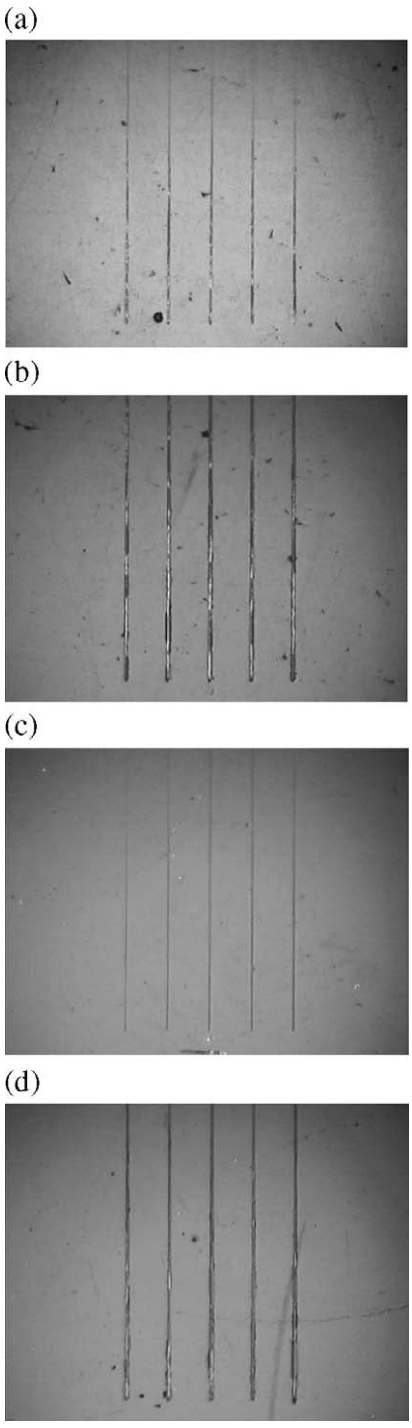


Fig. 7. Optical micrographs of scratch damages to the films: (a) a-C film deposited on untreated substrate at a maximum load of 10 mN, (b) a-C film deposited on untreated substrate at a maximum load of 30 mN, (c) a-C film deposited on $W^+$-implanted substrate at a maximum load of 10 mN, and (d) a-C film deposited on $W^+$-implanted substrate at a maximum load of 30 mN.

template between the steel substrate leading to structural continuity from the substrate to the film. In addition, it also acts as a buffer layer to eliminate stress concentration in the vicinity of the interface. The propagation and development of the cracks can be inhibited so that failure does not occur as easily compared to the untreated substrate. In addition, high energy ion implantation introduces radiation damage and C–C bonds act as a precursor for a-C film nucleation. Compared to the untreated substrate, the implanted surface possesses more nucleation sites that are beneficial to film growth. As shown in the optical micrographs in Fig. 7, more compact and higher-quality a-C films appear to have formed and they display better adhesion behavior in the scratch tests. The observed enhancement in adhesion is believed to stem from the synergistic effects of both factors.

## 5. Conclusion

The adhesion strength between the deposited a-C film and stainless steel substrate can be improved by pre-implanting tungsten ions into the steel substrate prior to film deposition. This is due to the formation of a modified layer consisting of tungsten carbide (WC) and C. The chemical compatibility between carbon and tungsten plays an important role on the improvement of the adhesion strength. From the nano-scratch tests, the critical load can be increased from 13 to 20 mN by this method. The improvement is believed to be due to the improved hardness of the modified layer as well as radiation damage which increases the number of nucleation sites thereby benefiting the growth of the film.

## Acknowledgements

This work was financially supported by Hong Kong Research Grants Council (RGC) Competitive Earmarked Research Grant No. CityU 1120/04E and National Natural Science Foundation of China. No. 50271004.

## References

[1] B. Bhushan, Tribology and Mechanics of Magnetic Storage Devices, 2nd ed., Springer, New York, 1996.
[2] J. Robertson, Mater. Sci. Eng. Rep. 37 (4–6) (2002) 129.
[3] X.Y. Liu, P.K. Chu, C.X. Ding, Mater. Sci. Eng. Rep. 47 (2–4) (2004) 49.
[4] R.W.Y. Poon, K.W.K. Yeung, X.Y. Liu, P.K. Chu, C.Y. Chung, W.W. Lu, K.M.C. Cheung, D. Chan, Biomaterials 26 (15) (2005) 2265.
[5] S.C.H. Kwok, J. Wang, P.K. Chu, Diamond Relat. Mater. 14 (1) (2005) 78.
[6] L. Knoblauch-Meyer, R. Hauert, Thin Solid Films 338 (1999) 172.
[7] S. Logothetidis, C. Charitidis, Diamond Relat. Mater. 9 (2000) 756.
[8] I. Endler, A. Leonhardt, Diamond Relat. Mater. 5 (1996) 299.
[9] Z.M. Zeng, T. Zhang, X.B. Tian, B.Y. Tang, T.K. Kwok, P.K. Chu, Surf. Coat. Technol. 128–129 (2000) 236.
[10] P.K. Chu, S. Qin, C. Chan, N.W. Cheung, L.A. Larson, Mat. Sci. Eng. Rep. 17 (6–7) (1996) 207.
[11] P.K. Chu, B.Y. Tang, L.P. Wang, X.F. Wang, S.Y. Wang, N. Huang, Rev. Sci. Instrum. 72 (3) (2001) 1660.
[12] C. Charitidis, S. Logothetidis, Surf. Coat. Technol. 125 (2000) 201.
[13] D. Briggs, M.P. Seah, Practical Surface Analysis, Vol. 1, Second edition, John Wiley and Sons, 1993.
[14] C. Rincon, G. Zambrano, A. Carvajal, P. Prieto, Surf. Coat. Technol. 148 (2001) 277.
[15] K. Hamrin, G. Johansson, A. Fahlman, C. Nordling, J. Phys. Chem. Solids 30 (1969) 1835.
[16] L. Ley, M. Cardona, Y. Baer, M. Campagna, W.D. Grobman, Topics in Applied Physics, L.Ley and M.Cardona, Vol. 27, Springer-Verlag, Berlin Heidelberg New-York.

[17] N. Moncoffre, G. Hollinger, H. Jaferezic, Nucl. Instrum. Methods Phys. Res., B Beam Interact. Mater. Atoms 7/8 (1985) 177.
[18] J. Diaz, G. Paolicelli, S. Ferre, Phys. Rev. ,B 54 (11) (1996) 8064.
[19] A.S. Lim, A. Atrens, Appl. Phys., A 51 (1990) 411.
[20] J.H. Yang, T.H. Zhang, Vacuum 4 (2001) 11.
[21] J.H. Yang, T.H. Zhang, Mater. Sci. Eng., A Struct. Mater.: Prop. Microstruct. Process. 362 (2003) 200.
[22] L. Porte, Phys. Rev., B 28 (1983) 3214.
[23] K. Dyrda, M. Sayer, Thin Solid Films 355–356 (1999) 277.
[24] S.B. Hu, J.P. Tu, Z. Mei, Surf. Coat. Technol. 141 (2001) 174.
[25] K.-R. Lee, K.Y. Eun, Thin Solid Films 377–378 (2000) 261.